Photoreactors Design for Hydrogen Production

Gianguido Ramis[a*], Elnaz Bahadori[a], Ilenia Rossetti[b]

[a] Dip. Ing. Chimica, Civile ed Ambientale, Università degli Studi di Genova and INSTM Unit-Genova, Genoa, Italy
[b] Chemical Plants and Industrial Chemistry Group, Dip. di Chimica, Università degli Studi di Milano, Italy
 gianguidoramis@unige.it

The production of hydrogen through photoreforming of aqueous solutions of organic compounds is considered as a way to exploit solar energy storage in the form of hydrogen. The photocatalytic reforming can be promoted by a photocatalyst, optimally a solid semiconductor able to absorb the major quota of solar energy. In this work, glucose was used as a model substrate for photoreforming, possibly derived from the hydrolysis of waste biomass. The selected photocatalysts were based on TiO_2. The materials were prepared by different methods, *e.g.* flame spray pyrolysis, precipitation and in mesoporous form through soft template synthesis, and compared with commercial samples of nanostructured TiO_2 P25 by Evonik. 0.1 mol% Pt was also added as co-catalyst. The role of the metal was that of electron sink, to inhibit the recombination of the electron/hole couple obtained through light absorption.

The photoreforming reaction was carried out in different prototypes of photoreactors, specifically developed and optimised. In one reactor configuration, an external 200 W lamp was used, with emission wavelengths centred around 365 nm. A first photoreactor was developed with internal capacity ca. 0.3 L, with big head space for gas collection and very efficient mixing of the suspension thanks to an optimized length/diameter ratio (L/D) *ca.* 2. A drawback was the poor irradiation efficiency of the suspension, which limited the overall productivity, irrespectively or the substrate. A different home-designed photoreactor was equipped with an immersion lamp, coaxial with the reactor. Two reactor sizes were tested, 0.3 L or 1.5 L. A significant amount of H_2 was obtained with these very simple catalyst formulations, up to 14.7 mol kg_{cat}^{-1} h^{-1} over the Pt/TiO_2 sample and using glucose as substrate. This result is very remarkable with respect to conventional photoreactors.

1. Introduction

Nowadays, *ca.* 100 million metric tons of hydrogen are produced worldwide (Armaroli & Balzani, 2011), which is less than 3 % of the world's primary energy demand and more than 95% derives from fossil sources. A growing search for clean energy vectors, such as H_2, exploded in recent years, including the investigation on solar based production of hydrogen. The first photocatalytic method for H_2 production was the solar water splitting proposed by Fujishima and Honda in the 1970s (Fujishima & Honda, 1972). The main drawback is that this process is thermodynamically limited by the high Gibbs free energy required to split water into its constituting elements (237 kJ/mol = 1.23 eV) and the rapid recombination of the produced H_2 and O_2. This latter point introduces additional complications to photoreactors design, requiring separate compartments for the evolution of the two products, which increases the kinetic losses. The photocatalytic activity is based on the use of semiconductors that, upon irradiation with energy larger than the band gap, promote an electron from the valence to the conduction band. The efficiency of the catalyst strictly depends on its light-harvesting properties and on the capacity to preserve the hole/electron pair from recombination.

The oxidation of water by holes is by far the slowest half reaction, so a sacrificial organic compound is often added, called Hole Scavenger (HS). Besides accelerating the reaction, a further advantage is that CO_2 is formed from HS oxidation instead of O_2, avoiding its recombination with H_2 and allowing the use of single compartment reactors. This route is conventionally called photoreforming (PR) and finds a particularly interesting application when waste organics are used as HS. The general stoichiometry is the following:

$$C_xH_yO_z + (2x - z)\, H_2O \rightarrow x\, CO_2 + (2x - z + y/2)\, H_2 \tag{1}$$
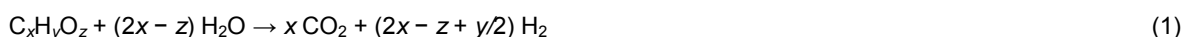
PR can be used to clean waste water derived *e.g.* from food, wine or paper industry (Linsebigler & al. ,1995; Gomathisankar & al., 2016; Rossetti, 2012) using solar energy and coupling H_2 production as an added value. TiO_2 is the semiconductor most used in photocatalysis because it is widely available, non-toxic and inexpensive, though its efficiency is very poor with solar radiation since it absorbs in the UV range, which constitutes *ca.* 5 % of the solar spectrum. TiO_2 has been used in this work, prepared by different methods, *i.e.* in dense nanoparticles form through flame spray pyrolysis (FSP (Chiarello & al., 2007a; Chiarello & al., 2007b), in microporous form by precipitation, in mesoporous form by soft template synthesis (Freyria & al., 2017) and compared with a commercial nanostructured compound (Evonik P25). Glucose has been used as a model molecule to represent the case of carbohydrates rich solutions obtained by hydrolysis of waste cellulose or lignocellulosic biomass.

While considerable attention is devoted to the development of innovative photocatalysts, the investigation on the role of the photoreactor and light distribution inside it is much lower (Heggo & al., 2017; Ola & Maroto-Valer, 2016; Rossetti & al., 2017; Rossetti & al., 2018). To contribute to fill this gap, we have compared the performance of three reactors for the photoreforming of glucose over a commercial TiO_2 catalyst. The effect of the lamp location in the reactor (co-axial immersed lamp or external irradiation from top) and of different TiO_2 samples was investigated, considering H_2 productivity and organics conversion.

2. Materials and experimental apparatus

Photocatalysts

Aeroxide TiO_2, P25 (Evonik) is one of the most used types of titania for its high activity. P25 is composed by anatase (78-85 %) and rutile (14-17 %) phases, plus an amorphous phase (0-13 %) (Ohtani & al., 2010). The specific surface area (SSA) is *ca.* 48 m^2/g and the particle size is nanometric (< 100 nm).

A mesoporous titania sample (called *meso*) was prepared by sol-gel from two solutions: Solution (A), prepared by drop-wise addition of 5.0 g $Ti(OBut)_4$ to 30.0 mL of an aqueous solution of acetic acid (20 vol%) and by vigorous stirring for about 4h at room temperature (r.t.); Solution (B), obtained by mixing 3.0 g Pluronic P123 and *ca.* 20.0 mL ethanol. Then the solution (B) was added to the solution (A) using a dropping funnel. The obtained mixture was sealed and stirred for 24 h at r.t, then left in an oven at 85 °C for 48 h inside a Teflon autoclave. The precipitate was filtered, dried at 80 °C and calcined at 450 °C in air for 4 h (Freyria & al., 2017). A comparative microporous sample (named *prec*) was prepared by precipitation of $TiOSO_4 \bullet xH_2SO_4 \bullet yH_2O$ in NaOH followed by calcination at 400 °C in airflow (Trevisan & al., 2014).

Flame spray pyrolysis is an innovative technique to synthesize high surface area solid oxides in a single step. The apparatus is extensively described elsewhere (Compagnoni & al., 2016) and essentially is based on a home-developed burner, fed with 4.4 mL/min of the oxide precursor solution and with 5 L/min of oxygen. The pressure drop at the burner nozzle is set at 1.5 bar. TiO_2 (named *FSP*) was produced from titanium isopropoxide as precursor dissolved in a volumetric flask with o-xylene and propionic acid (Chiarello & al., 2007a; Chiarello & al., 2007b).

Pt was loaded on the P25 sample by wet impregnation. The semiconductor (3 g) was suspended in milliQ water under vigorous stirring. Then the desired amount of metal precursor (Pt acetylacetonate, ≈ 15 mg) was added, corresponding to 0.1 mol%. The solution was kept under stirring at r.t. for 2 h and then the solvent was removed by evaporation at reduced pressure (40 °C). The collected powder was dried in an oven at 100 °C overnight and then reduced in a tubular oven at 700 °C under flowing H_2. A preliminary Temperature Programmed Reduction experiment determined the reduction temperature.

The structure of the catalysts was characterised by XRD (Phillips P3020), the textural properties by adsorption/desorption of N_2 at 77 K (Micromeritics ASAP2020), the band gap was estimated by DR-UV-Vis (Perkin Elmer Lambda35).

Photoreactors and testing conditions

For this work, three different types of photoreactors have been used (Figure 1). *Reactor #1:* AISI 316 stainless steel cylinder-shaped reactor with a cooling/heating jacked (Galli & al., 2017). Reactor volume is 1.7 L with a net capacity of 1.3 L. A co-axial quartz candle holds the UV lamp, a medium pressure 125 W mercury vapour lamp, emitting in the wavelength range between 254 and 364 nm. Lamp power is periodically checked using a photo-radiometer (Delta OHM HD2102.2), sensitive in the range 315-400 nm. The average irradiance measured during the time ranged from 150 to 175 W/m^2 during the testing campaign.
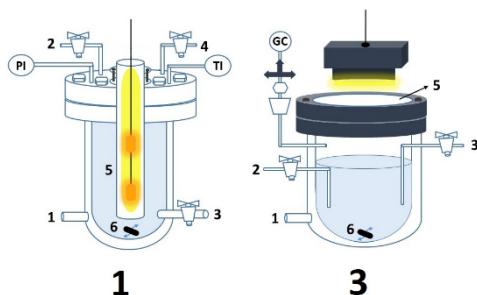
Figure 1: Photoreactors sketches.

Reactor #2: has a cylindrical shape with a heating/cooling jacket, with volume 300 mL and holds a co-axial lamp, similar to Reactor #1, but with one bulb only. It also has two branches: one for gas blowing that is directly connected to the helium line and for the manual liquid phase sampling; and the other one for gas output and gas phase analysis. The average irradiance measured was *ca.* 45 W/m^2.

Reactor #3: has the same structure and volume of Reactor #2, but it is irradiated from the top through a quartz window of 1 cm thickness, using a UVA lamp (Jelosil, HG 200 L) with maximum emission at 365 nm. The average irradiance measured was *ca.* 75 W/m^2, ranging from 50 to 100 W/m^2 depending on the distance from the lamp. All the reactors allowed gas inlet to remove air before the analysis and sampling places for the gas and liquid phase. A gas chromatograph (Agilent 7890) was used for the quantification of H_2, CH_4, CO, CO_2 and polar/non-polar light gases. COD - chemical oxygen demand - analysis was used to quantify the concentration of organic molecules in the sample through their complete oxidation with $K_2Cr_2O_7$ in an acidic environment at 130 °C for 30 minutes. The amount of reacted Dichromate, correlated to the residual organic fraction, is determined by spectrophotometric analysis of the produced Cr^{+3} ions with a Perkin Elmer Lambda 35 spectrometer at 605 nm. TOC - total organic carbon - analysis measured the organic carbon in the sample by its conversion into CO_2, then measured thanks to a detector (IR, FID or TCD). A Shimadzu Dry Combustion TOC was used, operating at 680 °C with a Pt supported catalyst.

The procedure to load the reactor was the same for all reactors, except the solution volume. The tests were carried out on 5 g/L solutions of glucose, after suspension of 0.25 g/L of the photocatalyst, setting the temperature at the desired value (80 °C for reactors #1 and #3, 60 °C for reactor #2) and degassing the system by bubbling inert gas for 30 min at r.t.. The sampling of the gas phase was carried out before the test to check the air elimination. The three samples of the liquid phase were used to assess the glucose concentration at time 0. Finally, the lamp is turned on for 5 h, sampling the gas phase sample every hour for GC analysis. At the end of the test three samples of the liquid phase were taken and analysed for organics conversion (by COD/Dry TOC).

3. Results and Discussion

Effect of Photocatalyst formulation

The differently prepared TiO_2 samples were characterized by different phases composition. In particular, both the samples prepared by flame synthesis, the home-prepared FSP and the P25 commercial one, were constituted of a mixture of the anatase and rutile phases, the latter more evident for sample FSP in reason of the higher preparation temperature, which can also explain the slightly bigger particle size. By contrast, both the Meso and Prec samples were constituted by the pure anatase phase, with very similar particle size. The SSA was comparable for the P25, FSP and Meso samples, while it was almost double for the catalyst prepared by precipitation due to microporosity. The addition of Pt by wet impregnation did not change the physical properties of the P25 sample appreciably, except some sintering due to the high-temperature reduction, while it significantly decreased the band gap from 3.3-3.4 to 3.1 eV. This can be attributed to a surface plasmonic contribution due to the metal.

Photocatalytic testing has been performed on the different samples and photoreactors according to a previously optimized protocol (Rossetti & al., 2015). Accordingly, a reaction temperature of 80 °C, the glucose concentration of 5 g/L and catalyst concentration of 0.25 g/L were selected for all tests, except with photoreactor #2, where the heating jacket allowed to stably fix the temperature up to 60 °C, only.

Two blank tests have been carried out, without the photocatalyst to exclude direct photolysis and under dark conditions to exclude a pure catalytic reactivity. In both cases, no H_2 production was observed. A third tests without glucose as HS excluded a significant effect of direct water splitting, H_2 productivity being not significant, though not nil.

Table 1: Main physical-chemical properties of the TiO$_2$ materials.

Sample	P25	FSP	Meso	Prec	Pt/P25
Anatase / Rutile (%)	78/22	65/35	100/0	100/0	87/13
Particle size (nm)	15	23	19	17	21
SSA (m^2 g^{-1})	45	67	57	114	55
Total volume of pores (cm^3 g^{-1})	0.11	0.14	0.07	0.45	0.32
Band Gap energy (eV)	3.41	3.31	3.41	-	3.12
Reduction temperature (°C)	-	-	-	-	700

Table 2: Photocatalytic testing for the photoreforming of glucose.

Reactor	Average irradiance (W/m^2)	Sample	H$_2$ productivity (mol/kg h)	C conversion (%)
#1	150-175	P25	1.910	20.3
#1	150-175	FSP	1.195	8.5
#1	150-175	Meso	0.918	-
#1	150-175	Prec	0.623	5.7
#1	150-175	Pt/P25	14.7	25.7
#2	45	P25	1.643	17.1
#3	75	Pt/P25	3.122	11.2

The productivity of H$_2$ was higher for the mesoporous sample (Meso) than for the microporous one (Prec), in spite of the much higher surface area of the latter. This was attributed to the larger pores size of the mesoporous sample, which allowed faster diffusion of the reactant and thus better catalyst utilization factor with respect to the microporous one. However, higher productivity was achieved with the P25 sample, followed by FSP. Their higher activity was attributed to the presence of two polymorphs of TiO$_2$, which allow a fast local charge transfer between anatase and rutile allowing charge segregation and the consequent increase of their lifetime. The FSP sample was less active due to the presence of some carbonaceous residue deriving from its preparation from organic precursors, which act as defects for charge recombination, lowering the activity.

The conversion of the carbonaceous substrate follows the same reactivity order. The products distribution for the different samples is reported in Figure 2, which shows that part of the carbonaceous skeleton of the substrate is mineralized by reforming to H$_2$ + CO/CO$_2$, while some C$_2$ product like C$_2$H$_4$ or C$_2$H$_6$ may evolve.
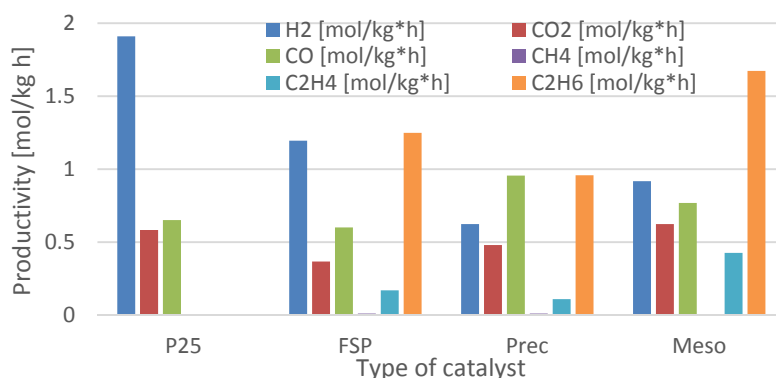

Figure 2: Products distribution for the comparison of different photocatalysts using Reactor #1.

If pure H$_2$ is needed, the best solution is, of course, the use of the P25 catalyst, but if the scope is the production of a gaseous fuel mixture, the possibility to exploit also ethane and ethylene allows to increase the efficiency of the process. Indeed, the amount of stored energy in the gas phase (calculated according to the Higher Heating Value of each compound (Green & Perry, 2008)) amounts to 167 kJ/h kg$_{cat}$ for the P25 catalyst, increasing to 2,440, 3,467 and 1,825 kJ/h kg$_{cat}$ for samples FSP, Meso and Prec, respectively.

The addition of 0.1 mol% Pt to P25 further boosted H$_2$ productivity to 14 mol/h kg$_{cat}$ that is one of the best results available in the literature for this reaction. The co-production of 0.303 mol/h kg$_{cat}$ of ethylene and 0.952 mol/h kg$_{cat}$ of ethane was also visible, for a total 6,113 kJ/h kg$_{cat}$ energy storage.

Effect of reactor design

Different photoreactors have been compared for this reaction. Reactor #1 has a cylindrical shape, holds ca. 1.3 L of suspension and has a co-axial immersion lamp. Reactor #2 shares with #1 the same geometry and diameter length ratio, but has lower capacity, 0.3 L. The smaller size of reactor #2 suggests the use of a lower power of the lamp to avoid overheating (ca. 45 W/m^2 average irradiance to be compared with more than 150 W/m^2 of reactor #1) and taking advantage to the location of the suspension nearer to the light source.

Reactor #3 is instead characterized by an external lamp, located on the top of the reactor. This configuration imposes a mono-directional irradiation top-down, with an intensity almost linearly decreasing with the distance from the source. External irradiation is believed typically as less effective than the internal one, but it is more easily amenable to scale up and use with natural irradiation with solar light.

Testing of sample P25 in reactor #2 returned 14 % lower productivity of H$_2$ than with reactor #1, but with a 70 % reduction of the irradiance. Therefore, the shorter optical path in reactor #2 was the key to guarantee an overall high efficiency of this photoreactor. On the other hand, reactor #3 led to ca. 3 mol/h kg$_{cat}$ of H$_2$ productivity for sample 0.1 mol% Pt/TiO$_2$, with respect to 14.7 mol/h kg$_{cat}$ obtained with reactor #1, in line with a less efficient light distribution through longitudinal irradiation with respect to the radial one. Also, in this case, the lamp power was halved for reactor #3 (75 W/m^2) with respect to reactor #1, but the decrease of productivity was much worse than the decrease of irradiance. Thus, in order to increase the effectiveness of the photoreactor, the optimization of the light distribution pattern and the distance from the source prevail over the use of an intense light source. The efficiency of the process can be quantified by two indexes. Efficiency 1 has been calculated from the Higher Heating Values (HHV) of all the compounds, products and reactant (Green & Perry, 2008). It represents the percentage of the original energy content of glucose, stored as gaseous fuel after the photocatalytic treatment. This kind of efficiency allows comparing the valorization of valuable compounds as such or as substrates for photoreforming, provided that the reactant can be exploited valuably in different ways. This is probably not the case of waste organic-containing solutions, but may fit the hydrolysis of raw biomass that can be valorized elsewhere. Efficiency 2, instead, represents the percentage of the irradiating power stored in the gas phase products. Both the parameters are reported in Table 3.

Table 3: Efficiency of energy storage as gas phase products.

Reactor	Sample	H$_2$ prod. (mol/kg$_{cat}$ h)	C$_2$H$_4$ (mol/kg$_{cat}$ h)	C$_2$H$_6$ (mol/kg$_{cat}$ h)	Stored energy (kJ/kg$_{cat}$ h)	Efficiency 1 (%)	Efficiency 2 (%)
#1	P25	1.91	-	-	546	4.3	0.39
#1	FSP	1.195	0.107	1.249	2287	18.1	1.62
#1	Meso	0.918	0.426	1.672	3262	25.8	2.31
#1	Prec	0.623	0.109	0.958	1708	13.5	1.21
#1	Pt/P25	14.7	0.303	0.952	5997	47.4	4.24
#2	P25	1.643	-	-	470	21.2	4.58
#3	Pt/P25	3.122	-	-	893	61.4	35.11

The overall amount of stored energy depends on products distribution, remaining below 1 MJ/h kg$_{cat}$ when the only fuel produced in the gas phase is H$_2$, to much higher values when also C$_2$ products are present. Efficiency 1 also depends on the products distribution and, for the same reactor #1, sharply increases when C-containing byproducts are exploitable in the gas phase. When only H$_2$ is present, only 4.3 % of the energy of the substrate is recovered after 5 h in the gas phase, notwithstanding the highest productivity of catalyst P25 for H$_2$. Likely longer reaction time would be needed to fully convert to remaining organic compounds in the liquid phase. The efficiency dramatically improved with the Pt-promoted sample, reaching almost 50% of the original heating power of the reactant recovered as product. Efficiency 2 follows substantially the same trend and reaches a maximum of stored power of ca. 4.2 %. This result is of course not economically valuable for an artificially irradiated photoreactor, but it can turn into a satisfactory goal if (free) solar energy can be exploited in the same way. The same efficiency was obtained with reactor #2 by using a much cheaper commercial photocatalyst, while the highest value was achieved with reactor #3. This exceptionally high efficiency, in spite of lower H$_2$ productivity, is explainable from the small area subject to irradiation (one order of magnitude lower than for the other two reactors), but it is anyway interesting to exploit future reactor designs with much larger windows, thus enhancing light exposure.

4. Conclusions

The photoreforming of glucose has been studied as a route for the production of H$_2$ from solar energy and the valorisation of waste or biomass-derived aqueous streams. Different catalyst formulations were tested, the highest productivity being achieved with the 0.1 mol% Pt/P25 photocatalyst, reaching ca. 15 mol/h kg$_{cat}$

productivity of H_2, which is an excellent result compared with the literature values, which are typically < 2 mol/h kg_{cat} (Montini et al., 2016). Glucose conversion and hydrogen productivity also depended on the design of the photoreactor. Higher productivity was achieved with coaxial immersion lamps, in particular by reducing the optical path through the reacting suspension. However, interesting productivity, yet lower, has been observed with a top irradiated photoreactor, which exhibited the highest efficiency in the utilisation of the lamp power. This suggests further modifications of the design in this configuration, which is easily amenable to be applied with natural irradiation, by enlarging the exposed surface.

Acknowledgments

References

Armaroli N., Balzani V., 2011, The hydrogen issue, ChemSusChem. 4, 21–36.

Chiarello G.L., Rossetti I., Lopinto P., Migliavacca G., Forni L., 2007, Solvent nature effect in preparation of perovskites by flame pyrolysis. 1. Carboxylic acids, Appl. Catal. B: Environmental, 72, 218.

Chiarello G.L., Rossetti I., Lopinto P., Migliavacca G., Forni L., 2007, Solvent nature effect in preparation of perovskites by flame pyrolysis. 2. Alcohols and alcohols + propionic acid mixtures, Appl. Catal. B: Environmental, 72, 227.

Compagnoni M., Lasso F.J., Di Michele A., Rossetti I., 2016, CO2 photoconversion to fuels, Catal. Sci. & Technol, 6, 6257.

Freyria F.S., Compagnoni M., Ditaranto N., Rossetti I., Piumetti M., Ramis G., Bonelli B., 2017, Both pure and Fe doped mesoporous titania catalyse the oxidation of Acid Orange 7 by H2O2 in different experimental conditions, Catalysts, 7, 213.

Fujishima A., Honda K., 1972, Electrochemical Photolysis of Water at a Semiconductor, Nature, 238, 37

Galli F., Compagnoni M., Vitali D., Pirola C., Bianchi C, Villa A., Prati L., Rossetti I., 2017, CO2 photoreduction at high pressure to both gas and liquid products over commercial titanium dioxide, Appl. Catal. B, 200, 386.

Gomathisankar P., Kawamura T., Katsumata H., Suzuki T., Kaneco S., 2016, Photocatalytic hydrogen production from aqueous methanol solution using titanium dioxide with the aid of simultaneous metal deposition, Energy Sources, Part A Recover. Util. Environ. Eff. 38, 110–116.

Green D.W., Perry R.H., 2008, Perry's Chemical Engineers' Handbook, Eighth Edition, McGraw-Hill.

Linsebigler A.L., Lu G., Yates J.T., 1995, Photocatalysis on TiO2 Surfaces: Principles, Mechanisms, and Selected Results, Chem. Rev., 95, 735–758.

Montini T., Monai M., Beltram A., Romero-Ocaña I., Fornasiero P.,2016, H2 production by photocatalytic reforming of oxygenated compounds using TiO2-based materials, Mater. Sci. in Semiconductor Proc., 42, 122–130.

Ohtani B., Prieto-Mahaney O.O., Li D., Abe R., 2010, what is Degussa (Evonik) P25? Crystalline composition analysis, reconstruction from isolated pure particles and photocatalytic activity test, Journal of Photochemistry and Photobiology A: Chemistry, 216, 179-182.

Ola and Maroto-Valer., 2016, Chem. Eng. J, 283, 972-978.

Rossetti I., 2012, Hydrogen Production by Photoreforming of Renewable Substrates, ISRN Chem. Eng. 2012, 1–21.

Rossetti I., Villa A., Compagnoni M., Pirola C., Prati L., Ramis G., Wang W., Wang D., 2015, CO2 photoconversion to fuels, Catal. Sci & Technol, 5, 4481.

Rossetti I., Compagnoni M., Ramis G., Freyria F., Armandi M., Bonelli B., 2017, Chem. Eng. Trans., 57, 319.

Rossetti I., Bahadori E., Compagnoni M., Tripodi A., Villa A., Prati L., Ramis G., 2018, Conceptual design and feasibility assessment of photoreactors for solar energy storage, Solar Energy, 172, 225-231.

Trevisan V., Olivo A., Pinna F., Signoretto M., Vindigni F., Cerrato G., Bianchi C.L., 2014, C-N/TiO2photocatalysts: Effect of co-doping on the catalytic performance under visible light, Appl. Catal. B Environ. 160–161, 152–160.